



NVH SIGNAL ANALYSIS VIA PATTERN RECOGNITION ANNS: AUTOMOTIVE BRAKE CREEP GROAN AS CASE STUDY

Manuel Pürscher, Stefan Schöpf, Peter Fischer

Institute of Automotive Engineering (office.ftg@tugraz.at), Graz University of Technology, Austria

Abstract: Automotive Noise, Vibration and Harshness (NVH) issues often cause costly customer complaints. In particular, NVH of the brake system is critical for subjective ratings of vehicle safety and passenger comfort. Recently, especially a stick-slip induced low-frequency phenomenon, the so-called brake creep groan, has become increasingly relevant. In order to avoid this brake NVH problem within upcoming automobile fleets, simulative and/or experimental parameter studies throughout all industrial brake development stages are indispensable. To this end, reasonable and efficient data analysis methods are necessary too. This kind of signal assessment challenge is addressed here by means of a method which applies techniques of Artificial Intelligence (AI) or Artificial Neural Networks (ANNs) respectively. The basis for this is a large number of generically synthesised brake component acceleration spectra which represents data in the frequency domain with and without creep groan. This generic data is used to create specifically elaborated pattern recognition ANNs. Eventually, the proposed approach provides an integrated framework of conditioned ANNs which is supposed to detect and separate non-linear signatures of different brake creep groan vibrations. In order to examine the method's practical limitations, additional data sets of synthetic accelerations including generic noise have been considered, and moreover, gauged accelerations concerning two test rig setups have been taken into account. Although the devised creep groan analysis approach is designated for automotive brake development workflows, its principle could be appropriate for similar NVH problems or signal analysis tasks in other engineering fields alike.

Key words: artificial neural networks, brake vibrations, creep groan, pattern recognition, signal analysis, stick-slip

1. INTRODUCTION

1.1. Automotive Brake NVH

For some years now, the automotive industry has been facing immensely increasing requirements for technical, economical, environmental and people-oriented aspects for a manifold range of ever faster developed vehicle types. This also counts for automotive Noise, Vibration and Harshness (NVH) issues which are potentially misconstrued by drivers and passengers as serious quality deficits, or even as system malfunctions. Hence, automotive NVH requirements involve inherently safety-critical friction brake systems in particular.

Beyond aspects related to car occupants exclusively, offer sound-emitting brakes annoyance potential for external individuals too. Akay [1] mentioned a survey from the 1930s which stated brake noise as a top-ten urban noise pollution problem of New York City. Nowadays, in case of up-to-date (semi-) automated vehicle driving modes such as *Parking-Pilot* or *Garage-Pilot*, an externally affected person could even be the actual "driver", see Fig. 1 and [2] respectively.

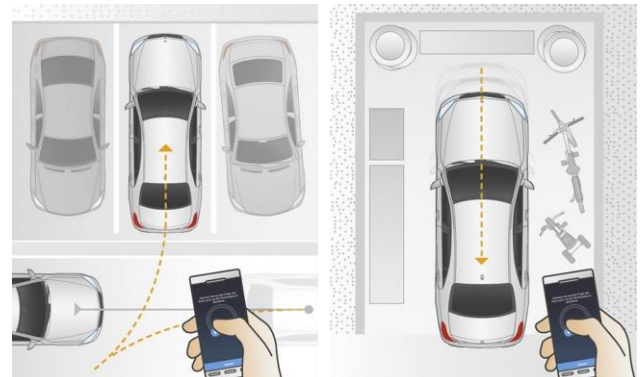


Fig. 1. *Parking-Pilot / Garage-Pilot* enable remote operability by external "driver", adapted from [2].

However, brake NVH affected the subjective perception of a car's and/or brand's comfort and reliability long before advanced technologies such as those just referenced entered the market. In 1991, Crolla and Lang [3] presented research data concerning reported brake faults after the market launch of five different European passenger car series. For each up to 1-year-old type, brake noise was indicated with a dominant quantity. In the early 2000s,

Akay [1] referenced to industry studies which assessed annual costs of brake NVH warranty claims on the North American market around one billion dollar. According to a paper of Abendroth and Wernitz [4] from the same period, leading automotive friction material companies spend almost 50 % of their engineering budgets directly or indirectly on measures against brake NVH problems. A few years later, Bittner [5] mentioned a comparable cost component for the automotive brake system supplier as a whole. A *J.D. Power Studies* North American market survey from 2014 [6], which rested upon more than 40.000 responses by original owners of up to 3-year-old automobiles, yielded two different brake NVH problems within the top-five complaints. A Japanese market study from 2017 [7] reported NVH of friction brakes as a major inconvenience for around 2 % of roughly 19.000 involved purchasers.

Thus, vibro-acoustic friction brake emissions entail an undesirable circumstance of high priority. One of these, the so-called brake creep groan phenomenon, is in focus within this article. In the typical automotive (disk) brake NVH classification chart in Fig. 2, which is based on an adapted literature condensation including [5] by Huemer-Kals [8], one can imagine via the sensibility examples in [9] that self-excited creep groan is situated in the tactile/audible frequency range of human perception.

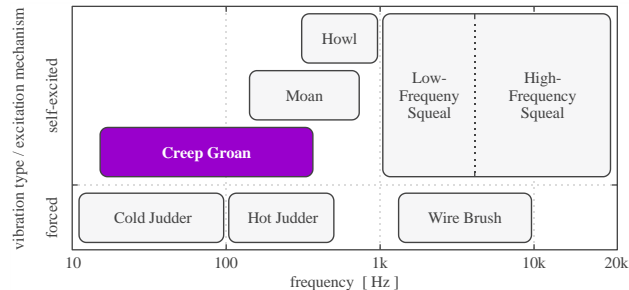


Fig. 2. Typical classification of common (disk) brake NVH phenomena, adapted from [8].

A comparable verbalised classification can be found in [10]. Although further fragmentation in terms of brake NVH is possible, e.g. 10 spectral and/or phenomenological subdivisions in [9], or even 15 terminologies in [1], the creep groan issue remains one of the most salient ones.

According to the typical distribution of warranty claims, which has been outlined graphically by Barton and Fieldhouse [10] based on the report of a high performance vehicle manufacturer, it owns the third largest share. Independent of that exemplary claim distribution, creep groan has a steadily increasing relevance for all commonly installed brake types and chassis designs within all vehicle segments due to several reasons such as described hereafter.

1.2. Topicality and Phenomenology of Creep Groan

The main reasons for a growing attention towards the creep groan issue are an increased customer expectation in conjunction with a reduced vibro-acoustic background sound level of advanced engines and powertrains. Therefore, creep groan is problematic for high-priced and/or electrified passenger cars with disk brake systems in particular. Nevertheless, it is also present for drum brakes and/or commercial vehicles which is pointed out in a publication by Karabay et al. [11]. Their work includes market surveys, value and failure analyses as well as troubleshooting measures concerning a specific light truck.

Various creep groan phenomena of all systems have comparable origination situations with associated characteristic spans of certain operational parameters in common. Accordingly, the brake pressure is moderate and a very slow vehicle velocity near standstill is present, whereby the occurrence of creep groan is favoured from cold and/or wet environments in particular. Since the mentioned simultaneity of both operational parameters is in some (semi-) automated driving modes a potentially mandatory situation for safety reasons, e.g. for remote controlled parking or during activated stop-and-go driver assistance features, creep groan tends to become progressively more relevant within automobile fleets of the next decade. However, concerning previous vehicles with standard automatic gearboxes it has been a known, but often secondarily treated brake NVH problem.

Oscillation characteristics of creep groan phenomena with mechanical and tribological component influences have not only been outlined in former works of the authors, e.g. [12, 13, 14], but also in specific book chapters and in studies of other research groups, e.g. [9, 10, 11]. Accordingly, creep groan is related to a physically unstable triggering mechanism which is in tribology fields described as stick-slip effect. This self-excited process at the main friction interfaces leads to periodic non-linear low-frequency brake and chassis vibrations with large component deflections. Accompanying short-term structure-borne noise disturbances appear inside and outside the car with relevant contents up to 500 Hz.

1.3. AI and ANNs for Pattern Recognition

More and more companies have started to see real-life benefits of Artificial Intelligence (AI) implementations. Early adopters of AI are mainly from sectors with a data-driven background such as the financial service industry or the automotive area, e.g. concerning stock trading or in terms of low-frequency interior noise evaluation [15]. Beyond such initial adopters, is nowadays a wide range of strongly digitalised business sectors just

like complex technology fields supported by assorted varieties of AI, as outlined by Bughin et al. [16].

A typical application of AI is machine learning with pattern recognition as one of its major branches. Rosenfeld and Wechsler [17] summarised historical perspectives and expected future directions of pattern recognition within their article almost 20 years ago. They described pattern recognition as one of the most important functionalities for intelligent behaviour which is displayed in biological and artificial systems alike. A prominent biological example is the detection of foreign intruders in an organic body by specific cellular antibodies in order to ensure the host's survival. For man-made tasks, a prepared AI seeks to apply approximating functions with the lowest possible probabilities of misallocations for the evaluated data set. Thus, the pattern recognition problem is akin to the more general issue of statistical regression. Typical artificial use cases are optical character readers to comprehend and separate written letters or text modules, biometrical algorithms to identify persons by means of fingerprints, iris, face or speech, and furthermore, medical analysers to find anomalies in heart electrocardiograms. Liu et al. [18] have listed further application fields such as linguistics, meteorology like exemplarily shown in [19], philosophy, psychology, robotics, or even very specialised areas, e.g. ethology. They traced the latest progresses especially to recent technology trends such as social computing.

However, modern mathematical/empirical functions for pattern recognition rest upon Artificial Neural Networks (ANNs). According to [15, 17, 19, 20], two coherent data sets are necessary in order to obtain the requested functionalities. For so-called supervised learning, these are input signals (variables) which are available in the functions' development procedure as well as in the later application, and furthermore, output targets (variables) which are usually known in the set-up process exclusively.

1.4. Problem Definition / Aim of Study

Creep groan phenomena are challenging for automotive NVH engineers. In view of this circumstance, innovative investigation methods and industrially implementable routines are necessary. These should help to devise and optimise efficient remedial technical measures in upcoming vehicle development projects. For this purpose, the authors have already published concepts of new experimental and/or simulative methods, e.g. [12, 13, 14].

It is only natural that comprehensive creep groan investigations, which lead to a vast amount of data, require reasonable and efficient data assessment tools. This kind of signal analysis task is addressed here via an innovative creep groan classification method based on pattern recognition ANNs.

1.5. Article Structure

Representative brake component acceleration signals of creep groan appearances, which were recorded with two different setups in similar operational parameter studies at corner test rig level, are discussed in section 2. The idea behind the simplification of characteristic creep groan signatures in order to synthesise a high amount of more or less realistic acceleration frequency spectra generically is presented in chapter 3. These specifically synthesised data sets are used to develop differently elaborated pattern recognition ANNs which are content of section 4. Then, a data set of synthetic spectra including noise is processed to check the well-considered framework of conditioned ANNs. In addition, sets based on measured acceleration data get involved to assess the framework's capabilities in a more realistic way. Both verification strategies with previously unseen spectra are discussed in section 5. Summary and conclusion of the new application method are drawn in chapter 6. Eventually, prospects on feasible refinements and further research steps are content of section 7.

2. REPRESENTATIVE CREEP GROAN SIGNATURES

2.1. Corner Test Rig Experiments with Two Setups

Typical signatures of creep groan vibrations are discussed here via brake component acceleration signals. The accelerations were gauged at the disk brake callipers of two dissimilar automobile front corner setups. Design models of these excluding the wheels are shown true to scale together in Fig. 3 and [14] respectively.

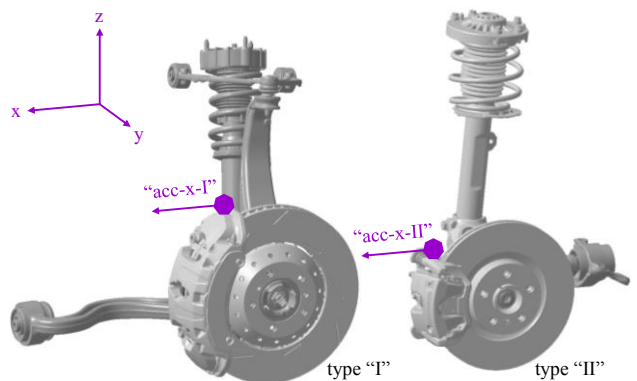


Fig. 3. Calliper accelerometer positions "acc-x-I" and "acc-x-II" on front corner systems type "I" and type "II", adapted from [14].

The design on the left, named type "I", belongs to a sporty grand tourer, whereas type "II" on the right illustration is implemented in a compact van. As one can see, type "I" follows the double wishbone suspension principle with fixed calliper brake module. Type "II" on the right is built

with a MacPherson suspension assembly including floating calliper brake construction. Both setups had, among other sensors, a miniature triaxial accelerometer glued to the upper surface of the calliper. Nevertheless, only the signals according to vehicle x-direction, named "acc-x-I" and "acc-x-II", are actually of relevance.

Creep groan of both setups was investigated at a drum driven suspension and brake test rig. It is pictured with an exemplary front corner setup of the left vehicle side in Fig. 4 and [14] respectively.



Fig. 4. Drum driven suspension and brake test rig for creep groan parameter matrix experiments, adapted from [14].

Information about the test rig's sophisticated structure with adaptable functionalities as well as its interface constructions for the mounting of automobile corners, and furthermore, the test rig's capabilities regarding main operational parameters and basic environmental conditions under control can be found in [12]. The previous work also describes an innovative systematic creep groan investigation approach with its well-defined sensitivity experiments in detail. This test matrix procedure leads to rather extensive acceleration data sets. Basically, these data sets allow comparisons of defined combinations of brake pressure and drum (vehicle) velocity for different mechanical and/or tribological component variants.

The two mentioned operational parameters were gauged and adjusted via the test rig's control management with a given rate of 100 Hz, whereas "acc-x-I" and "acc-x-II" have been recorded separately with 10 kHz.

2.2. Calliper Acceleration Signal Patterns

In the following, a diagram with an acceleration recording including its computed Fast-Fourier-Transform (FFT) is presented for each of three distinctive brake creep groan vibrations of type "I" and type "II" respectively. The FFT with an upper calculation limit adjusted to 2 kHz applies a Hanning window of 50 % overlap to an 1 s time segment

which contains the depicted short segment of 0.18 s in each case. This results in an appropriate frequency resolution of exactly 1 Hz up to the practically chosen boundary of 1 kHz.

Detailed explanations of creep groan phenomena with extensive interpretations of similar self-measured calliper accelerations have already been documented in [12, 13, 14]. Apart from that, Akay [1] showed and explained comparable time plots and frequency spectra related to other friction-induced vibration mechanisms.

The two diagrams without creep groan show comparable acceleration patterns, see Fig. 5 and Fig. 6. It makes no difference that dissimilar setups were tested regarding opposed oriented drum rotations with velocities unequal by the factor 4. Thus, both comparable time signals contain low fluctuations which are just related to small corner setup oscillations as well as subordinate test rig vibrations and/or unproblematic measurement noise. A FFT leads to spectra with flat broadband bumps and relatively low and narrow decibel (dB) peaks.

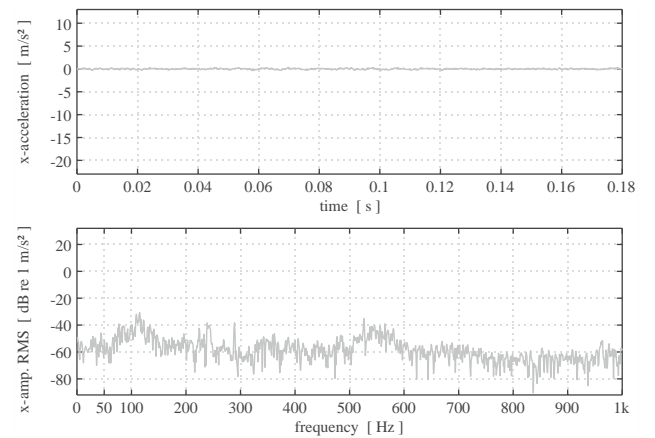


Fig. 5. Acceleration "acc-x-I" without creep groan, 4 bar / 0.04 km/h.

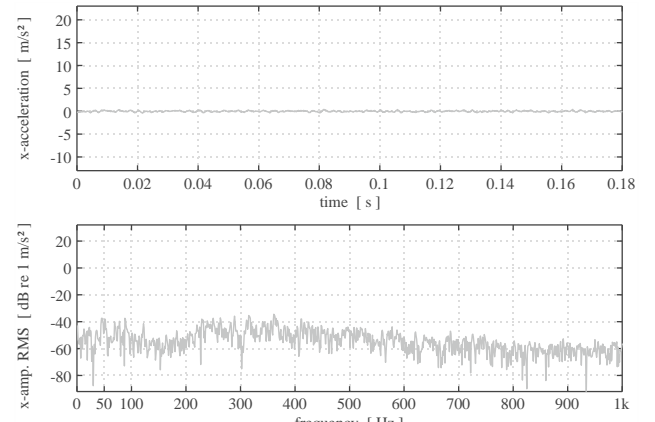


Fig. 6. Acceleration "acc-x-II" without creep groan, 4 bar / -0.16 km/h.

The two typical examples of creep groan within the deeper frequency area, depicted in Fig. 7 and Fig. 8, reveal strong accelerations with more or less pronounced non-linear characteristics.

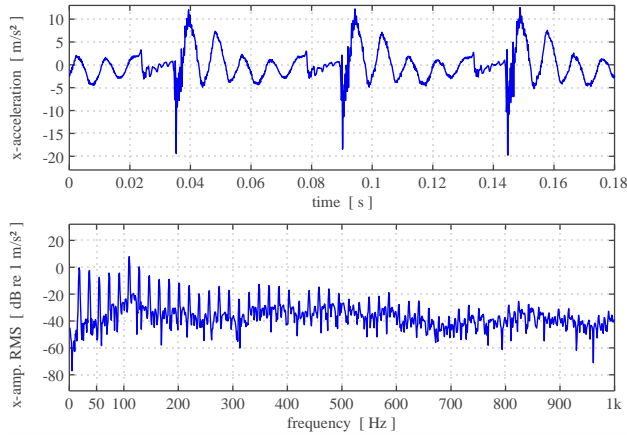


Fig. 7. Acceleration “acc-x-I” with 18 Hz creep groan, 10 bar / 0.16 km/h.

Therefore, the characteristic spectral behaviour is found to be an appropriate criterion within the introduced AI approach. Accordingly, the observable regular patterns of the spectra are of relevance.

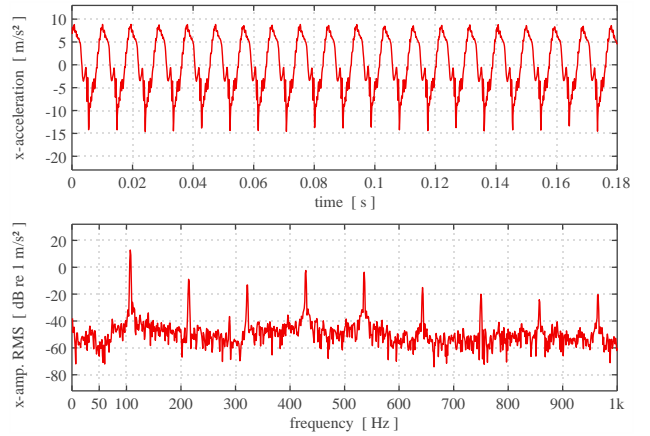


Fig. 9. Acceleration “acc-x-I” with 107 Hz creep groan, 7 bar / 0.08 km/h.

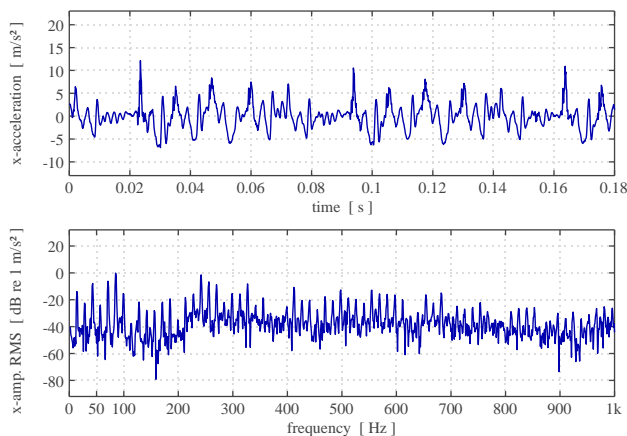


Fig. 8. Acceleration “acc-x-II” with 14 Hz creep groan, 10 bar / -0.04 km/h.

Moreover, the two calliper x-accelerations concerning creep groan vibrations within the upper frequency area, shown in Fig. 9 and Fig. 10, also represent distinctive non-linear signatures.

All four acceleration time data plots have a relatively steep and rather high amplitude (amp.) peak which is followed by some less intense fluctuations or damped natural oscillations respectively. This striking signal pattern repeats accurately with a specific interval according to the dominant stick-slip transition. The tribological switch-over appears in the shown instances with 18 Hz, 14 Hz, 107 Hz and 86 Hz respectively. If applying a FFT on such kind of periodic non-linear signal, prominent Root Mean Square (RMS) dB peaks of usually different heights will result at multiple intervals of the basic frequency. This can be seen in the spectra of all four creep groan phenomena.

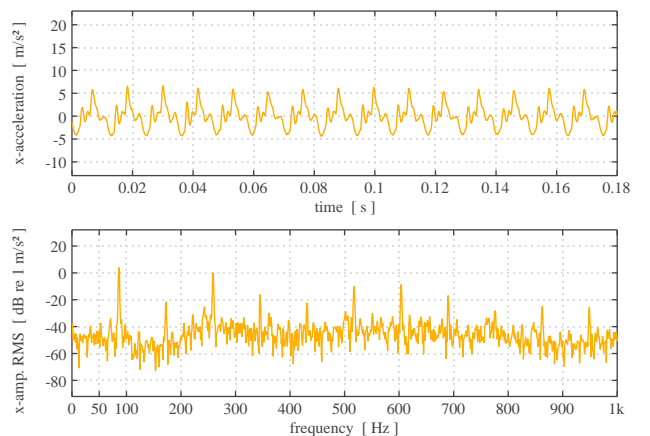


Fig. 10. Acceleration “acc-x-II” with 86 Hz creep groan, 7 bar / -0.08 km/h.

All shown instances of “acc-x-I” and “acc-x-II” refer to differently combined operational parameters which were representatively chosen out of the existing test matrices. Further comparable experimental and/or simulative creep groan signatures regarding both setups can be found in [12, 13, 14]. The related master thesis by Huemer-Kals [8] contains additional experimental examples.

2.3. Operational Parameter Sensitivity Studies

Although friction at micro- and macroscopic scale with respect to vibro-acoustic effects has been intensively studied by many authors, e.g. reviewed in [1], there are open questions on specific friction-induced mechanisms in various engineering fields. To a certain extent, this applies to the non-linear behaviour of creep groan vibrations. However, the systematic investigation

approach published in [12] enables already a better detection of other non-linear influences apart from the evident tribological interface, e.g. those of axle elastomer bushings. Therefore, changing subsystem oscillations with specific component participations are also identifiable.

The non-linear influences due to operational parameter variations can be recognised in the form of zonally switching basic creep groan frequencies in the so-called Creep Groan Map (CGM). It was introduced in [12] with 190 operational parameter combinations of brake pressure and drum velocity. An adapted CGM with merely 49 test matrix entries and reduced complementary information is illustrated in Fig. 11 for type "I" and in Fig. 12 for type "II" respectively.

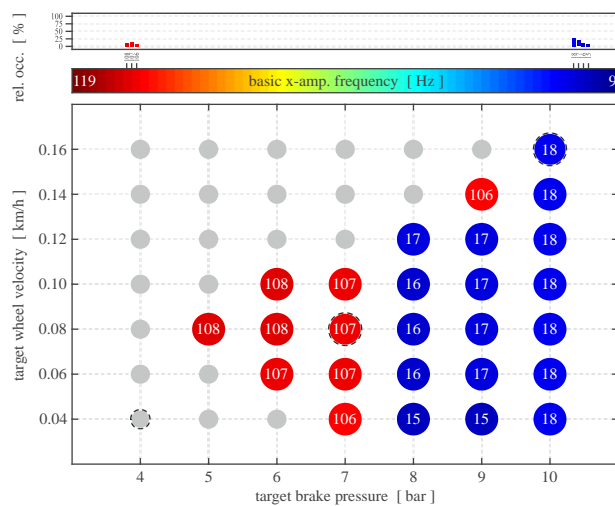


Fig. 11. CGM of type "I" with 49 test matrix entries of brake pressure / forward drum velocity.

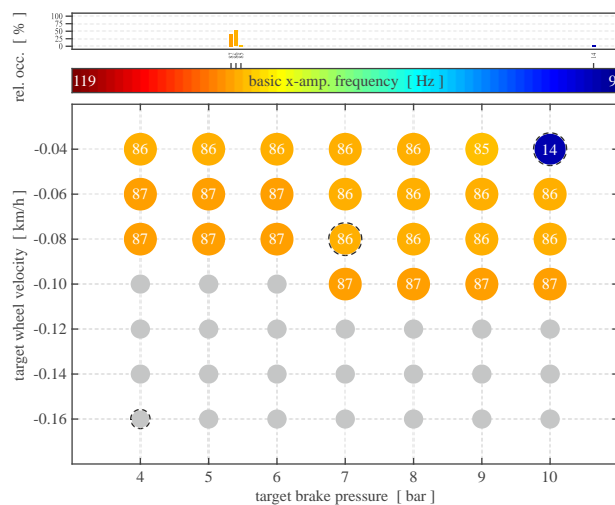


Fig. 12. CGM of type "II" with 49 test matrix entries of brake pressure / reverse drum velocity.

Both evaluations are based on comparable operational parameter spans with identical brake pressures regarding

opposed drum rotations. As one can see, each chart reveals two different frequency areas for the basic stick-slip interval which is indicated via a certain colour and the corresponding numeric frequency value. Moreover, a relative occurrence (rel. occ.) of each enabled basic frequency is reported. Since comparable frequency areas have evinced for all automobile front corner setups tested so far, the adjusted frequency window between 9 Hz and 119 Hz results just from the authors' experience. A presence of two prominent stick-slip frequency areas in each CGM becomes especially clear, if brake pressures higher than 10 bar are considered, compare to [12, 13]. Nevertheless, the shown test matrices contain all relevant subsystem interactions which are potentially activated during creep groan appearances. Note that the previously discussed x-acceleration examples are bordered with dotted circles.

In order to derive a CGM, the evaluation algorithm presented in [12] is applied. It rests upon spectral analyses with well-considered adaptable queries. Thereby, the method is fairly well able to distinguish x-accelerations with creep groan vibrations from those without. As depicted before, the deterministic algorithm is also intended to categorise the basic frequency of creep groan. Because only if it is determined, the brake NVH issue is treatable holistically. Of course, also super-harmonic spectral contents of the friction-induced excitation are examinable via the algorithm. In prospective development steps, source-drain properties towards a passenger's perception, according to a vibro-acoustic chain of effects such as pictured by Marschner et al. [9], might be calculated and improved. Independent of that vision, an evaluation of the exact frequency contents supports the interpretation of design benchmarks and/or material studies and gives feedback on potentially switching subsystem interactions from the upper to the deeper frequency area or vice versa.

Nevertheless, reliability and accuracy of the currently applied deterministic evaluation method suffer, if fuzzy acceleration time signals such as depicted in Fig. 8 appear, or even if the adaptable queries are improperly chosen. The proposed AI approach aims to deliver step-by-step advancements in order to overcome these present deficiencies. Whether and how this is realisable is under investigation within this study.

3. GENERIC SYNTHESIS OF ACCELERATION DATA SETS

3.1. Functionality Set-Up: Input Signals / Output Targets

Besides the capabilities of the *Pattern Recognition app* within the *ANN Toolbox* provided by *MATLAB R2016a*, the presented approach's principle rests upon comprehensive data sets of different acceleration frequency spectra in

particular. These are relevant to generate an integrated framework of 112 autarchic ANNs (see also chapter 4.2.) in total.

Since not enough measurements regarding possible creep groan manifestations (between 9 Hz and 119 Hz) were available in order to do so, an acceleration generation formalism has been designed. It evolved from subjective inspections of hundreds of frequency spectra with and without creep groan vibrations. Additionally, it has similarities to the evaluation algorithm proposed in [12]. As hinted, the generic formalism enables a reproducible creation of extensive data sets of synthetic x-accelerations or input spectra respectively. To this end, typical creep groan signatures are simplified via 10 adjustable spectral attributes which are visualised in Fig. 13.

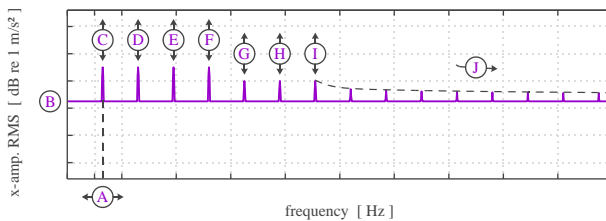


Fig. 13. Attributes of the generic spectra.

By means of these well-considered attributes, 112 separate data sets of input signals have been processed. Of course, related output targets were defined alike. It should be noted that the basic concept in terms of synthesised data sets for the elaboration of pattern recognition ANNs has already been followed in the broad area of automotive NVH, e.g. by Lee and Chae [15].

The so-called “primary-ANN” (see also chapter 4.4.) deals with the basic frequency categorisation. It refers to a reproducible data set of 242.757 input spectra. The 111 so-called “secondary-ANNS” (see also chapter 4.5.), which are meant for creep groan judgement, are based on 82.944 reproducible input spectra per relevant basic creep groan frequency. All synthetic x-acceleration signals have a frequency resolution of 1 Hz up to the useful boundary of 1 kHz. The demanded acceleration amplitude peaks are achieved via addition of super-harmonic in-phase sine oscillations below a given limit of 1 kHz. To this end, a time domain resolution of 10 kHz is provided and the basic frequency of the fundamental sine wave is varied stepwise from 9 Hz to 119 Hz. The superimposition is followed by a FFT similar as described in the previous chapter. Thus, all equally spaced peaks are realistically supported from adjacent frequencies. An adaptable bandwidth of white noise as well as an amplitude attenuation, which diminishes super-harmonic orders above an initial attenuation frequency equal to the seventh acceleration amplitude peak with 1 dB/octave, are both implemented in the frequency domain.

The values for each of the 10 spectral attributes used to compile the 242.757 unique input spectra for the only “primary-ANN” can be extracted out of Table 1. Note that eight of these attributes are actually varied.

index	attributes									
	↔(A)↔	(B)	↑(C)↓	↑(D)↓	↑(E)↓	↑(F)↓	↑(G)↓	↑(H)↓	↑(I)↓	↔(J)↔
variable [unit]	basic frequency [Hz]	white noise [↗ ↘]	x-amp. RMS [dB re 1 m/s ²]						x-amp. RMS attenuation [dB/octave]	
minimum	9	-35 (no)	-30	-30	-30	-30	-30	-30	-30	-1
increment	1	–	20	20	20	20	10	10	10	–
maximum	119	–	10	10	10	10	-10	-10	-10	–
input spectra (1 Hz ... 1 kHz)										
values [#]	per attribute	111	1	3	3	3	3	3	3	1
cumulative - all	111	111	333	999	2.997	8.991	26.973	80.919	242.757	242.757
... - frequency	1	1	3	9	27	81	243	729	2.187	2.187

Table 1. Attributes of 242.757 generic input spectra to obtain one “primary-ANN” for basic frequency categorisation.

As one can read on the right side of the lowest table row, 2.187 spectrum options per creep groan frequency are available. This quantity is broken down in the listed combinatorial calculation. In the following, four examples illustrate the considered amplitude range limits. Fig. 14 shows the two borderline cases of all 9 Hz input spectra and Fig. 15 those of 119 Hz respectively. Even though both instances at the lower range would not be rated as creep groan vibrations in the end, it has no relevance for the determination of a basic frequency which is the exclusive task of the “primary-ANN”.

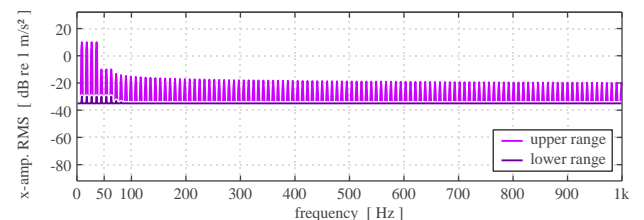


Fig. 14. Amplitude range limits of 2.187 generic input spectra to describe 9 Hz basic frequency.

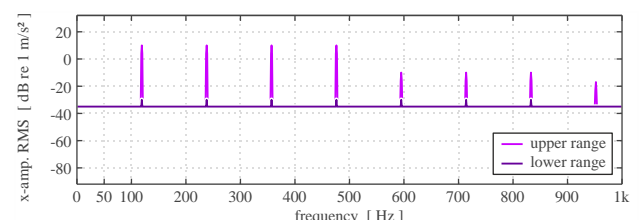


Fig. 15. Amplitude range limits of 2.187 generic input spectra to describe 119 Hz basic frequency.

The values for each of the 10 attributes used to compile the 9.206.784 singularly combined input spectra for the 111 alternative “secondary-ANNS” can be seen in Table 2.

Once again, merely eight of these spectral attributes are actually varied.

		attributes									
index		↔(A)	(B)	↑(C)	↓(D)	↑(E)	↓(F)	↑(G)	↓(H)	↑(I)	↔(J)→
values	variable [unit]	basic frequency [Hz]	white noise [→]	x-amp. RMS [dB re 1 m/s ²]					x-amp. RMS attenuation [dB/octave]		
	minimum	9	-35 (no)	-26	-26	-26	-26	-27	-27	-27	-1
	increment	1	—	—	—	—	—	—	—	—	—
	level I	—	—	-21	-21	-21	-21	-22	-22	-22	—
	level II	—	—	-19	-19	-19	-19	-18	-18	-18	—
	level III	—	—	-14	-14	-14	-14	—	—	—	—
	level IV	—	—	-4	-4	-4	-4	—	—	—	—
	maximum	119	—	6	6	6	6	-13	-13	-13	—
input spectra (1 Hz ... 1 kHz)											
options [#]	per attribute	111	1	6	6	6	4	4	4	1	
	cumulative - all	111	111	666	3.996	23.976	143.856	575.424	2.301.696	9.206.784	9.206.784
	... - frequency	1	1	6	36	216	1.296	5.184	20.736	82.944	82.944

Table 2. Attributes of 9.206.784 generic input spectra to obtain 111 autarchic “secondary-ANNS” for creep groan judgement.

The attribute values are different compared to those of Table 1. On one hand, tighter range limits for the x-acceleration amplitude peaks are taken into account here in order to create more realistic input spectra. On the other hand, the relevant attribute values have smaller increments in unequal intervals which results from an intended relation to the original evaluation algorithm introduced in [12]. However, this input signal mixture is supposed to provide “secondary-ANNS” which are able to recognise the requested regularities of creep groan vibrations within typical acceleration spectra.

Basically, at least one consistent output target formulation is necessary if an ANN for pattern recognition is elaborated. In case of the “primary-ANN”, each equivalent output target contains the prescribed information about the associated spectrum’s embedded basic frequency. This is realised via an 111 times 242.757 data matrix containing zeroes or ones, whereby a correct column entry is indicated by means of the value one. By contrast, the 111 output target data matrices used to define the “secondary-ANNS” have the sizes 2 times 82.944 respectively. The unique value one in a first column entry implies absence of creep groan for the related input spectrum. The single value one in the second column entry indicates contrary terms. Eventually, creep groan is prescribed in each of the 111 equivalent set-up data clusters for approximately 55 % of the input signals which is not a mandatory share.

3.2. Functionality Check: Unseen Noisy Verification Signals

In order to examine operability and capability of the designed framework with 112 self-sufficient ANNs at a

later stage, also a generic verification data set is designed. Its mixture made of 909.312 unique input signals is gathered in Table 3.

		attributes									
index		↔(A)	(B)	↑(C)	↓(D)	↑(E)	↓(F)	↑(G)	↓(H)	↑(I)	↔(J)→
values	variable [unit]	basic frequency [Hz]	white noise [→]	x-amp. RMS [dB re 1 m/s ²]					x-amp. RMS attenuation [dB/octave]		
	minimum	9	-35 (no)	-25	-25	-25	-25	-25	-25	-25	-1
	increment	1	—	10	10	10	10	10	10	10	—
	maximum	119	5	5	5	5	-15	-15	-15	-15	—
	evaluation spectra (1 Hz ... 1 kHz)										
	per attribute	111	4	4	4	4	4	2	2	1	
	cumulative - all	111	444	1.776	7.104	28.416	113.664	227.328	454.656	909.312	909.312
	... - frequency	1	4	16	64	256	1.024	2.048	4.096	8.192	8.192

Table 3. Attributes of 909.312 generic verification spectra including different white noise bandwidths to check framework of 112 ANNs.

The chosen attribute values are meant to be different compared to those of Table 1 and Table 2. Even though this applies neither to the described basic frequencies of the first column nor to the considered amplitude attenuation of the last column, there are still previously unseen verification spectra provided for the purpose of AI examination. This is even more true in view of three optional bandwidths of white noise superimposed to each of the 227.328 unique synthetic spectra, see Fig. 16.

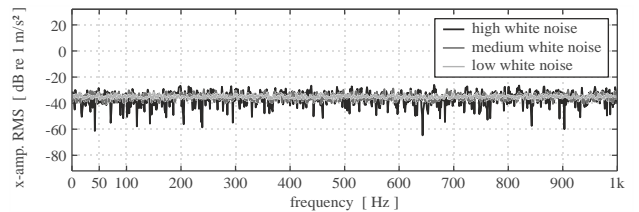


Fig. 16. Optional white noise variants superimposed to 227.328 generic verification spectra.

Each reproducible white noise spectrum is adjusted up to a limit of 1 kHz in order to reach a summarised overall RMS of 25 dB re 1 m/s² respectively. This also counts for the initial option without noise at all. Independent of that, the procedure to obtain the output targets concerning the more or less noisy verification signals is the same as discussed in the prior section. Note that output target values related to Table 3 are only necessary to examine the predictions of the proposed AI approach.

4. ELABORATION OF PATTERN RECOGNITION ANNS

4.1. Basic Model and Practical Implementation

As explained in the fundamental book of Hertz et al. [20], the basic scheme of a multilayer feed-forward pattern

recognition ANN commonly contains a passive input layer which is followed by a number of active hidden layers and a mostly active output layer in the end, see model in Fig. 17 and literature sources [15, 19, 20].

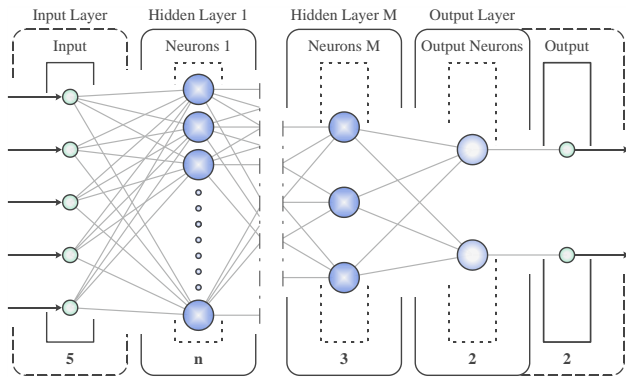


Fig. 17. Exemplary multilayer feed-forward ANN model, adapted from [15, 19, 20].

In simple terms, the number of hidden layers determines whether the ANN adapts the philosophy of either shallow or deep learning, whereby this distinction is not strictly defined. Each of these hidden layers accommodates a manually predefined amount of the substantial neurons, see neuron model explanations in [15, 20]. Accordingly, the neurons of the first hidden layer receive a stimulating signal via the input variables, manipulate the obtained values pursuant to specific inherent functions and then forward differently weighted values to the neurons of the next hidden layer or to those of the output layer respectively. If this output layer is active, the values get altered once more. The obtained result is a list of confidence values for each prescribed output variable.

It should be noted that the external connectors at input layer and output layer are often equivalently named input neurons and output neurons or just simply input and output, and furthermore, neurons are sometimes designated as nodes just like layers as units. A couple of these specialised terms are used within the referenced works [15, 17, 19, 20].

During an ANN's creation procedure, each active neuron's specific function is continuously adapted in order to minimise misallocations. For the topical implementation, this prefabricated process refers to supervised learning which means that output targets with preferable solutions are available for a comparison to predictions of the ANN. Of course, this pertains to the available algorithm for training/validation/testing in particular.

ANNs implemented within this work have been created by means of several modified scripts derived from the *Pattern Recognition* app within *MATLAB R2016a*.

Due to high data volumes provided for the creation process, out-of-memory issues appeared for the authors' premature plan to combine all set-up data clusters simultaneously in order to build one comprehensive ANN with abilities in basic frequency categorisation as well as creep groan judgement. However, this data volume problem of *MATLAB R2016a*, which was running here on *Windows 10 Pro 64 Bit* either at a *dual core i7* or at a *quad core i7* including 8 GB RAM respectively, has already been resolved by the software's developers via the so-called tall arrays. These allow the additional use of out-of-memory data, see description in [21] concerning more recent software releases. Nevertheless, the faced data volume restrictions made a workaround necessary.

4.2. Integrated Framework of 112 ANNs

The workaround is based on the separation of basic frequency categorisation and creep groan judgement. Therefore, an integrated framework including one "primary-ANN" and 111 autarchic "secondary-ANNS" has evolved. Due to this strategy, the memory requirements for training/validation/testing were strongly reduced. Certainly, the overall data volume was approximately the same, or even larger. However, the framework's task distribution and information flow can be seen Fig. 18.

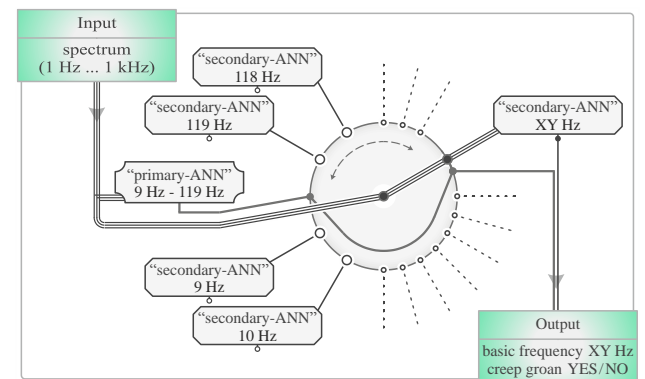


Fig. 18. Task distribution and information flow within framework of 112 self-sufficient ANNs.

Accordingly, the framework input reads a spectrum. It has a more or less embedded basic frequency which should be detected via the "primary-ANN" based on the highest of 111 probabilities. After this initial categorisation is done, the developed script routine forwards the spectrum to the "secondary-ANNS", whereby only the previously determined one is executed. It computes a probability approximation for both only possible states which means presence of creep groan or no occurrence. After all, the framework output includes the most likely stick-slip frequency of the imported spectrum and its related state concerning creep groan.

4.3. Split of Set-Up Data for Training/Validation/Testing

The “primary-ANN” is based on an 1.000 times 242.757 input signal data matrix and an 111 times 242.757 output target data matrix, whereas the other 111 autarchic “secondary-ANNS” rest upon 1.000 times 82.944 input signal data matrices and 2 times 82.944 output target data matrices. All 112 separate set-up data clusters were separately processed one after the other within the functionality generation phase.

Therefore, a well-considered split of each data matrix affiliation according to training/validation/testing was necessary. Eventually, a training data package is used to adapt an ANN in order to let it comply with as many known output targets as possible with respect to given input signals. A validation data package is mainly applied in terms of generalisation of an ANN. It is necessary to systematically decide whether and/or when to stop training. This leads to a ranking of the varied designs. Moreover, testing is important to independently quantify the effectiveness of an ANN’s concluded design on previously unseen set-up data packages. Thus, it becomes feasible to avoid unfavourable data memorisation effects.

In order to ensure a comparability of different versions and parameter settings, the initial set-up data split is done here via a predetermined index and not randomly.

4.4. “Primary-ANN” for Basic Frequency Categorisation

The “primary-ANN” is modelled with one hidden layer including 80 neurons of function type *tan-sigmoid* which is described in [15]. The data matrices of the already mentioned input signals and output targets determine the amount of 1.000 passive input neurons and 111 *softmax* function output neurons. This structure is shown in Fig. 19 based on the standardised ANN visualisation provided by the *Pattern Recognition app*.

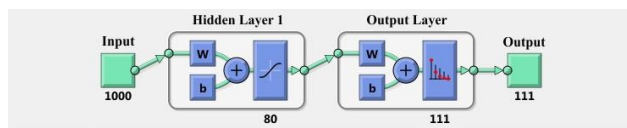


Fig. 19. Refined MATLAB representation for “1000-80-111” structure of the “primary-ANN”.

A percentual set-up data division of 80/10/10 for training/validation/testing and a regression value of 0.1 within the well-considered Scaled Conjugate Gradient (SCG) backpropagation training method, which is treated in [19], have been applied.

Compared to other options, the applied data split in combination with the mentioned regression value seem to deliver the best results while avoiding over-fitting on

the given set-up data clusters. The main reason to choose SCG over other equally well performing training techniques is its memory efficiency. This correlates with the findings of Azhar Omar et al. [19] concerning an ANN for meteorological issues.

The built-in stop criteria for training of the “primary-ANN” were set to 2.500 epochs, which is the maximum number of design iterations allowed for the entire layer composition, and moreover, to a limit of 500 consecutive validation checks which do not show improvements compared to the previously best. Only these two criteria are activated here in order to end the training iterations of the “primary-ANN”.

The final training cycle of the “primary-ANN” results in less than 1 % misclassifications, if considering the testing data package not used for training or validation. Basically, all attempted layer compositions and optional parameter settings were varied largely automated until no further significant improvements regarding the minimisation of misclassifications occurred.

4.5. “Secondary-ANNS” for Creep Groan Judgement

Each of the 111 self-sufficient “secondary-ANNS” contains two hidden layers including 120 *tan-sigmoid* neurons respectively. The sizes of the data matrices according to Table 2 lead to the amount of 1.000 passive input neurons and two *softmax* output neurons. The consistent structure of each “secondary-ANN” is shown abstractly in Fig. 20.

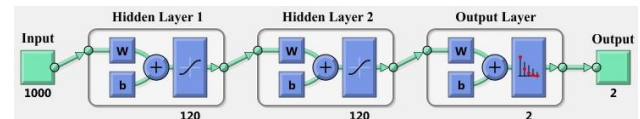


Fig. 20. Refined MATLAB representation for “1000-120-120-2” structure of each “secondary-ANN”.

In light of positive experiences, the percentual set-up data split for training/validation/testing was adjusted to 80/10/10 alike, and moreover, the SCG backpropagation training method and a regression value of 0.1 were chosen again.

An extension from one towards two hidden layers, which can be interpreted as adaption from a shallow to a deep learning philosophy, was necessary due to a former share of around 20 % misjudgements on average, if considering the testing data package not used for training or validation. Based on trial and error, two times 120 neurons achieved good results for this problem, whereby computational times were reasonable compared to ANN compositions with more extensive hidden layer numbers and/or neurons. Thus, the mentioned errors regarding both only possible states, which means presence of creep

groan or no occurrence, were reduced within all 111 “secondary-ANNs” to less than 2 % on average.

In order to achieve this optimisation while keeping the computational effort reasonable, the built-in stop criteria for training of each autarchic ANN concerning creep groan judgement were set to the upper limit of 10.000 epochs or training cycles respectively, to the maximum threshold of 500 consecutive validation checks without refinements compared to the previously best, to a demanded performance value lower than 0.00015 in terms of a cross-entropy calculation with a regularisation value of 0.05, and furthermore, to the upper time limit of 2 hrs. An optional gradient criterion related to the performance value curve is not used in order to avoid premature stops at local minima.

The additional stop criteria compared to those of the ANN for basic frequency categorisation were considered to ensure a predictable and manageable creation time across all 111 implementations. Accordingly, the cumulative time for training/validation/testing of the finally chosen layer compositions and parameter settings was approximately 130 hrs. However, specific “secondary-ANNs” have been retrained due to significantly worse reliabilities than the majority of the others. This would make clear that the realised branched ANN approach allows a simple comparison of identically created ANNs with a quick retraining possibility, whereas this is more problematic in a single ANN architecture.

5. VERIFICATION OF NEW CREEP GROAN PATTERN RECOGNITION METHOD

5.1. Check via Noisy Synthetic Input Signals

In the first part of the verification, the four variants with 227.328 unique synthetic spectra in each case are of relevance, see Table 3. Certainly, all prescribed output targets per variant are considered alike. Hence, each singular spectrum has a proper basic frequency as well as a preferable state whether creep groan should be allocated or not. Eventually, the elaborated framework’s reliability is quantified here in terms of pro-rata misevaluations per basic stick-slip frequency between 9 Hz and 119 Hz.

On one hand, “creep groan - underrated” means that the negatively signed percentual share, which is always normalised to roughly 65 % of all 2.048 spectra at a certain stick-slip frequency, is not judged by the “secondary-ANN” as creep groan, although it should be.

On the other hand, the positive percentual value regarding “no creep groan - overrated” means that this share, which pertains to the other approximately 35 % of

all 2.048 spectra at a certain basic frequency, is evaluated by the AI as creep groan, although the prescribed output targets of the related unseen verification spectra suggest contrary terms.

Of course, this interpretation implies that the upstream “primary-ANN” performs very well. Indeed, concerning all four variants this counts for at least 99.70 % of the generic verification spectra, whereby the highest success rate is reached without white noise and the worst one with high white noise. Independent of that, the very small shares of incorrect basic frequency categorisations are primarily a result of misclassifications towards whole-numbered multiples or dividers, e.g. 9 Hz categorised as 18 Hz or vice versa. It should be noted that the ensuing judgement of a wrongly assigned “secondary-ANN” is possibly still correct in case of absent creep groan vibrations. However, the aftereffects based on errors of the “primary-ANN” are included in the four bar graphs hereafter.

The AI misevaluations regarding the generic data set without white noise are shown in Fig. 21. As it can be seen via the left-most cumulative bars which are differently scaled by the factor 7, there is around -0.22 % underrating and 4.97 % overrating for the entire verification data set. However, the reliabilities of the 111 “secondary-ANNs”, which affect both cumulative percentual values much more than the “primary-ANN”, are very specific. An almost negligible underrating does not appear above 35 Hz at all, whereas a widely more significant overrating tends to occur there instead in particular. By contrast, the tendency towards misevaluations of the subjacent frequencies is rather opposed, but with less intensity. Obviously, the basic frequencies with 10 Hz, 12 Hz, 20 Hz, 114 Hz, 118 Hz and 119 Hz are a few exceptions of that rough rule of thumb. Hence, these “secondary-ANNs” have potentially stronger biases than the majority of the others.

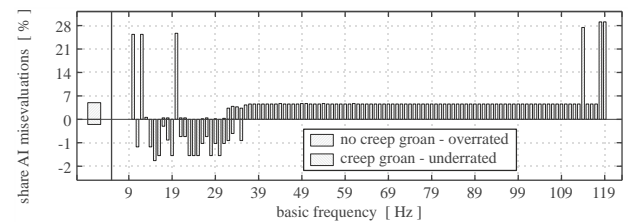


Fig. 21. AI misevaluations concerning 227.328 synthetic spectra without white noise.

The AI misevaluations regarding the generic data set with low white noise are broken down in Fig. 22. In general, there is a very similar distribution across the entire frequency window between 9 Hz and 119 Hz as discussed before via Fig. 21. Thus, low white noise is not an additional challenge for the framework of conditioned ANNs.

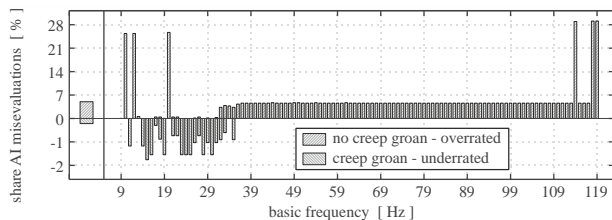


Fig. 22. AI misevaluations concerning 227.328 synthetic spectra including low white noise.

In comparison to both previous data sets, superimposed medium white noise leads already to slightly different verification results, see Fig. 23, whereby it is unfeasible to comprehend why just some basic frequencies are noteworthy affected. However, the main difference lies in an inferior success rate of the “secondary-ANNs” at 10 Hz, 22 Hz, 26 Hz, 45 Hz, 61 Hz, 70 Hz and 102 Hz. This leads to an average underrating of approximately -0.26 %. The opposite situation concerns around 5.17 %.

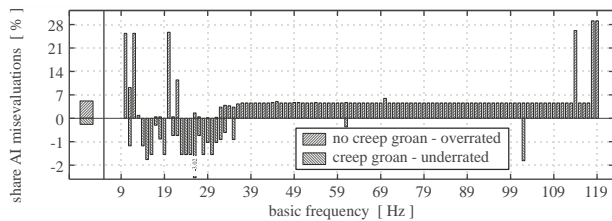


Fig. 23. AI misevaluations concerning 227.328 synthetic spectra including medium white noise.

Lastly, as indicated in Fig. 24, the synthesised data including high white noise leads to the largest percentual shares of misevaluations with rounded overall values of -0.56 % and 8.30 %. Once again, certain “secondary-ANNs” are more sensitive on noisy signal components than the majority of the others.

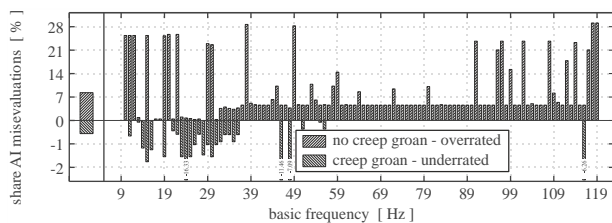


Fig. 24. AI misevaluations concerning 227.328 synthetic spectra including high white noise.

In summary, a clear bias towards overrating can be noticed within these four verifications. An interesting aspect is that “secondary-ANNs” with initially worst overrating, e.g. those of 10 Hz or 118 Hz, undergo no additional deterioration throughout all considered bandwidths of white noise.

5.2. Check via Measured Creep Groan Accelerations

In the second part of the verification, the integrated framework of conditioned ANNs is checked by means of measured calliper x-accelerations available from both automobile front corner test setups. Thus, the data sets applied for this are identical as discussed in section 2, and moreover, comparable visualisations as depicted in Fig. 11 and Fig. 12 can be generated. Hence, an AI-based CGM with 49 test matrix items is illustrated in Fig. 25 for type “I” and in Fig. 26 for type “II” respectively.

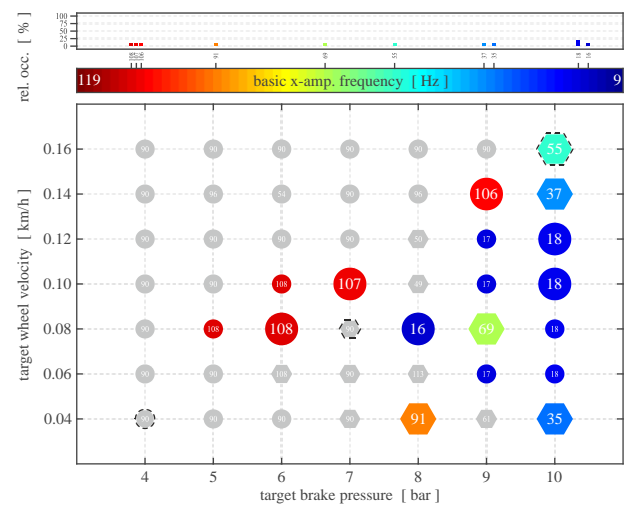
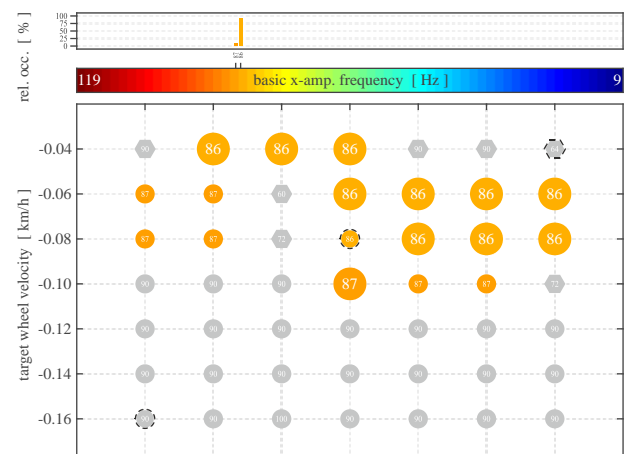


Fig. 25. AI-based CGM for test matrix of front corner system type “I”.



Colour-filled circles refer to appropriately assigned “secondary-ANNs” in case of actually present creep groan, whereby the large ones indicate its proper approval and the small ones its incorrect denial. Uniformly grey-shaded small circular areas represent the adequate rejection of creep groan in case of its actual absence which makes the included numeric values somehow dispensable. However, it is interesting that 90 Hz is assigned for most of these instances without creep groan vibrations.

Hexagons are used to illustrate faulty declared outputs of the “primary-ANN”. The larger ones in colour indicate a proper approval of creep groan. Unfortunately, always at inherently false basic frequencies. The smaller hexagons in grey show a false denial of creep groan. Even though it could be correct for wrongly assigned “secondary-ANNs”, these evaluation results are still errors in a holistic view.

Consequently, large coloured circles just like small grey ones are the only items that show the requested verification results in a similar manner as in the initial evaluations, compare to Fig. 11 and Fig. 12.

As one can see in Fig. 25 and Fig. 26, hypothetically correct test matrix entries are distributed rather patchy. Overall, around 59 % and roughly 71 % matches are reached. A further breakdown reveals that the “primary-ANN” performs appropriately for approximately 73 % of the considered test matrix x-accelerations of type “I”. For type “II”, this applies to about 86 % of the 49 items. Furthermore, the charts show that there is a conspicuous bias towards underrating of creep groan vibrations in case of correctly assigned “secondary-ANNs”, whereas overrating never occurred. Hence, all percentual values described most recently depend on the incidence of creep groan within the test matrix entries. Of course, this means that reliability and accuracy of the new evaluation approach are not objectively quantifiable based on measured creep groan accelerations.

6. SUMMARY AND CONCLUSION

This work’s main objective relates to the development of an integrated framework of pattern recognition ANNs in order to detect and separate potentially existing non-linear low-frequency brake creep groan vibrations within comprehensive measurements and/or simulations.

On one hand, the method rests upon several millions of generically synthesised acceleration spectra which feign data with and without creep groan more or less realistic.

The data sets have been synthesised in a well-considered manner after subjective analyses on thousands of available calliper acceleration spectra, see also examples in [12, 13, 14]. The frequency window for recognisable

basic stick-slip intervals of creep groan vibrations was adjusted from 9 Hz to 119 Hz. However, these are not mandatory values

On the other hand, the presented AI application method deploys the capabilities of the *Pattern Recognition app* within *MATLAB R2016a* in order to process the generic data in view of 112 self-sufficient ANNs in total.

However, only the faced data volume restrictions within this available software version led to the need for a workaround by means of these 112 autarchic ANNs in a branched architecture. In a positive sense, the distribution allows a simple comparison of identically created ANNs with a quick retraining possibility, whereas this would not be possible in a single ANN approach.

The so-called “primary-ANN”, which is used for basic frequency categorisation, has a form “1000-80-111”. By contrast, the other 111 so-called “secondary-ANNs”, which are used for creep groan judgement, are designed with more *tan-sigmoid* neurons and an additional hidden layer according to a form “1000-120-120-2” respectively.

Both multilayer feed-forward ANN types rest upon supervised learning, a reproducible index-based 80/10/10 percentual data division for training/validation/testing and a regression value of 0.1 in combination with the SCG backpropagation training function. Iteration stop criteria were adjusted within an automated training procedure in order to ensure reasonable computational times while avoiding premature stops.

As a whole, the computational times in terms of the finally chosen layer compositions and parameter settings including retraining of specific “secondary-ANNs” took nearly 200 hrs. Eventually, the final training cycles revealed for all 112 ANNs less than 2 % errors on average, if considering each testing data package not used for training or validation.

The framework’s practical limitations are determined by means of four additional synthetic acceleration spectrum compilations including different reproducible white noise bandwidths, and moreover, via two independent data sets of accelerations gauged for two typical passenger car front corner setups at a drum driven suspension and brake test rig. Thus, 909.312 generic verification spectra just like 98 measured ones have been considered in particular.

Each unique verification spectrum has a proper basic frequency and a preferable state whether creep groan should be allocated or not. Since these prescribed output targets are based on the deterministic creep groan evaluation algorithm presented in [12], which can be questioned critically on its own, there are uncertainties involved in case of fuzzy acceleration spectra in particular.

Nevertheless, it is assumed here that Fig. 11 and Fig. 12 reflect correct results.

In terms of all 909.312 generic verification spectra with a prescribed proportion of roughly 35 % absent creep groan, a tendency towards “no creep groan - overrated” can be noticed.

This overrating appears for 4.97 % to 8.30 % on average, whereas “creep groan - underrated” with respect to the other roughly 65 % counts for -0.22 % to -0.56 % on average. Both smaller values correspond to the data compilation without white noise and the larger values refer to high white noise respectively. The rounded overall success rates for these examples reach 98.12 % and 96.73 % respectively. Since the “primary-ANN” classifies at least 99.70 % of the spectra within each data set of the four synthetic verification variants very well, the major share of the emerged AI misevaluations can be traced to misjudgements of the “secondary-ANNs”.

A not fully understood aspect is that certain of these ANNs significantly change the reliability with increasing white noise bandwidths, whereas others do not show this behaviour, compare Fig. 21 with Fig. 24. Furthermore, it is interesting that underrating is rather omitted above 35 Hz.

In terms of the 98 examples of measured calliper x-accelerations with a known proportion of around 47 % absent creep groan vibrations, a clear bias towards underrating can be noticed via Fig. 25 and Fig. 26.

By contrast, overrating never occurred. The investigation shows that the “primary-ANN” performs adequately for approximately 80 % of the 98 considered test matrix items. Subsequently, the elaborated framework of conditioned ANNs reaches an overall hit rate of around 65 %.

However, a major concern in this verification part is the fact that these percentual values described most recently depend on the incidence of creep groan within the test matrix entries. Hence, a slightly higher overall hit rate of approximately 70 % is reached in case of considering both creep groan parameter matrices of [12] with 190 items respectively. On the downside, matches for the 190 test matrix items of [13] emerge only for roughly 37 %.

Based on verifications with these 570 additional items should be noted that potential for improvements seems to lie within a sophisticated treatment of typical misclassifications of the “primary-ANN”. These are often related to a detection of whole-numbered basic frequency multiples or dividers, and furthermore, to rounded basic frequency decimals which were not yet taken into account.

7. OUTLOOK

The developed approach’s principle rests upon not yet fully exploited capabilities of a specific software. Moreover, ANN models for pattern recognition can be adapted in many ways. Hence, more experienced software users and/or AI specialists probably detect potential for improvements. However, the fundamental set-up data clusters are always essential.

Millions of generically synthesised acceleration spectra have been considered. Nevertheless, there could be a lack of information in the attempt to imitate the evaluation algorithm introduced in [12]. Further attribute values might be tested or realistic spectral noise could be added, whereby a higher amount of generic input spectra for more training/validation/testing options should not be a main aim. Of course, the dimensions of the input signal data matrices might be reduced in order to decrease the computational effort, e.g. to 500 Hz.

Alternatively, measured creep groan accelerations could be considered during the set-up phase. Preliminary studies have shown a large potential with good matching rates around 90 % concerning this adapted single ANN strategy. Nevertheless, the available data pool from test rig measurements regarding different creep groan manifestations within the relevant frequency window is not yet enough. In view of upcoming creep groan experiments, or even with prospective transient simulations such as demonstrated in [13], this alternative approach with only one ANN is practicable at the soonest in a few years.

Lastly, it should be noted that the principle of the devised AI application method could be suitable for similar NVH problems or signal analysis tasks in other engineering fields alike. However, refinements have to be made in order to enable an implementation.

8. REFERENCES

- [1] A. Akay: **Acoustics of friction**, *The Journal of the Acoustical Society of America*, 111(4), 2002, 1525-1548, doi:[10.1121/1.1456514](https://doi.org/10.1121/1.1456514)
- [2] A.L. Dorofte: **The new Mercedes-Benz S-Class: The automotive benchmark in efficiency and comfort**, MERCEDES-BENZ / AUTOMOBILES / LIMOUSINE / S-CLASS, Mercedes-Benz-Blog, Bucharest, 2017, https://mercedes-benz-blog.blogspot.com/2017/04/the-new-mercedes-benz-s-class_19.html, accessed July 2018
- [3] D.A. Crolla and A.M. Lang: **Brake Noise and Vibration - The State of the Art**, *Tribology Series*, 18, 1991, Paper VII (i), 165-174, doi:[10.1016/S0167-8922\(08\)70132-9](https://doi.org/10.1016/S0167-8922(08)70132-9)

- [4] H. Abendroth and B. Wernitz: **The Integrated Test Concept: Dyno - Vehicle, Performance - Noise**, SAE Technical Paper 2000-01-2774, 2000, doi:[10.4271/2000-01-2774](https://doi.org/10.4271/2000-01-2774)
- [5] C. Bittner: **Reduzierung des Bremsenrubbelns bei Kraftfahrzeugen durch Optimierung der Fahrwerkslager**, Doctoral thesis, Technical University of Munich, Institute of Automotive Technology, Munich, 2006
- [6] J. Youngs: **Vehicle Dependability Study: Top 10 Problems in 3-Year-Old Vehicles**, *J.D. Power Studies*, J.D. Power, Westlake Village, 2014, <http://www.jdpower.com/cars/articles/jd-power-studies/vehicle-dependability-study-top-10-problems-3-year-old-vehicles>, accessed July 2018
- [7] G.O. Davies: **Vehicle dependability in Japan declines, J.D. Power finds**, *Automotive World*, Automotive World Ltd, Penarth, 2017, <https://www.automotiveworld.com/news-releases/vehicle-dependability-japan-declines-j-d-power-finds/>, accessed July 2018
- [8] S. Huemer-Kals: **Complex Eigenvalue Analysis of Friction Induced Low-Frequency Vibrations in Vehicle Disc Brake Systems**, Master thesis, Graz University of Technology, Institute of Automotive Engineering, Graz, 2018
- [9] H. Marschner, A. Pfaff, P. Leibolt and G. Maggi-Trovatoto: **Schwingungen und Geräusche**, 627-648, In: *Bremsenhandbuch*, B. Breuer and K. Bill (eds), 2017, Springer, doi:[10.1007/978-3-658-489-9_28](https://doi.org/10.1007/978-3-658-489-9_28)
- [10] D.C. Barton and J.D. Fieldhouse: **Noise, Vibration and Harshness (NVH)**, 255-317, In: *Automotive Chassis Engineering*, D.C. Barton and J.D. Fieldhouse (eds), 2018, Springer, doi:[10.1007/978-3-319-72437-9](https://doi.org/10.1007/978-3-319-72437-9)
- [11] S. Karabay, K. Baynal and C. İğdeli: **Detecting Groan Sources in Drum Brakes of Commercial Vehicles by TVA-FMEA: A Case Study**, *Strojniški vestnik - Journal of Mechanical Engineering*, 59(6), 2013, 375-386, doi:[10.5545/sv-jme.2012.809](https://doi.org/10.5545/sv-jme.2012.809)
- [12] M. Pürscher and P. Fischer: **Systematic Experimental Creep Groan Characterization Using a Suspension and Brake Test Rig**, SAE Technical Paper 2017-01-2488, 2017, doi:[10.4271/2017-01-2488](https://doi.org/10.4271/2017-01-2488)
- [13] M. Pürscher, S. Huemer-Kals and P. Fischer: **Experimental and Simulative Study of Creep Groan in Terms of MacPherson Axle Bushing Elasticities**, *Proceedings of EuroBrake 2018*, EB2018-SVM-011, May 22-24, The Hague, 2018
- [14] M. Pürscher, S. Huemer-Kals and P. Fischer: **Experimental Investigation of Low-Frequency Vibration Patterns in Automotive Disk Brake Systems: Utilization Study for Modal Simulation Methods**, SAE Technical Paper 2018-01-1513, 2018, doi:[10.4271/2018-01-1513](https://doi.org/10.4271/2018-01-1513)
- [15] S.K. Lee and H.C. Chae: **The application of artificial neural networks to the characterization of interior noise booming in passenger cars**, *Proceedings of the Institution of Mechanical Engineers, Part D: Journal of Automobile Engineering*, 218(1), 2004, 33-42, doi:[10.1243/095440704322829146](https://doi.org/10.1243/095440704322829146)
- [16] J. Bughin et al.: **Artificial Intelligence: The Next Digital Frontier?**, *McKinsey Global Institute Discussion Paper*, McKinsey & Company, 2017
- [17] A. Rosenfeld and H. Wechsler: **Pattern Recognition: Historical Perspective and Future Directions**, *International Journal of Imaging Systems and Technology*, 11(2), 2000, 101-116, doi:[10.1002/1098-1098\(2000\)11:2<101::AID-IMA1>3.0.CO;2-J](https://doi.org/10.1002/1098-1098(2000)11:2<101::AID-IMA1>3.0.CO;2-J)
- [18] H. Liu, J. Yin, X. Luo and S. Zhang: **Foreword to the special issue on recent advances on pattern recognition and artificial intelligence**, *Neural Computing & Applications*, 29(1), 2018, 1-2, doi:[10.1007/s00521-017-3243-x](https://doi.org/10.1007/s00521-017-3243-x)
- [19] M. Azhar Omar, M. Khair Hassan, A. Che Soh and M.Z.A. Ab Kadir: **Lightning severity classification utilizing the meteorological parameters: A neural network approach**, *Proceedings of 2013 IEEE International Conference on Control Systems, Computing and Engineering*, 111-116, Nov. 29 - Dec. 1, Minden, 2013, doi: [10.1109/ICCSCE.2013.6719942](https://doi.org/10.1109/ICCSCE.2013.6719942)
- [20] J. Hertz, A. Krogh and R.G. Palmer (eds): **Introduction to the Theory of Neural Computation**, 1991, Addison-Wesley, ISBN 0-201-50395-6
- [21] J. Little and C. Moler: **Matlab Release Notes**, *MATLAB Documentation*, The MathWorks, Inc., Natick, 2018, <https://de.mathworks.com/help/matlab/release-notes.html?rntext=&startrelease=R2017a&endrelease=R2018a&category=data-analysis&groupby=release&sortby=descending&searchHighlight=>, accessed August 2018